

RESEARCH ARTICLE

10.1002/2015JC011214

Key Points:

- The sources of sediment BC were apportioned by PMF receptor model merging with PAHs signatures
- Fossil fuels combustion was the dominant source of BC preserved in the BS and YS surface sediments
- BC subtypes and hydrodynamic conditions affected the spatial variations of fossil BC and biomass BC

Correspondence to:

Y. Chen,
yjchentj@tongji.edu.cn;
C. Tian,
cgtian@yic.ac.cn

Citation:

Fang, Y., Y. Chen, C. Tian, T. Lin, L. Hu, J. Li, and G. Zhang (2016), Application of PMF receptor model merging with PAHs signatures for source apportionment of black carbon in the continental shelf surface sediments of the Bohai and Yellow Seas, China, *J. Geophys. Res. Oceans*, 121, 1346–1359, doi:10.1002/2015JC011214.

Received 10 AUG 2015

Accepted 20 JAN 2016

Accepted article online 25 JAN 2016

Published online 15 FEB 2016

Application of PMF receptor model merging with PAHs signatures for source apportionment of black carbon in the continental shelf surface sediments of the Bohai and Yellow Seas, China

Yin Fang^{1,2,3}, Yingjun Chen^{1,2}, Chongguo Tian², Tian Lin⁴, Limin Hu⁵, Jun Li⁶, and Gan Zhang⁶

¹Key Laboratory of Cities' Mitigation and Adaptation to Climate Change in Shanghai, China Meteorological Administration, College of Environmental Science and Engineering, Tongji University, Shanghai, China, ²Key Laboratory of Coastal Environmental Processes and Ecological Remediation, Yantai Institute of Coastal Zone Research, Chinese Academy of Sciences, Yantai, China, ³University of Chinese Academy of Sciences, Beijing, China, ⁴State Key Laboratory of Environmental Geochemistry, Guiyang Institute of Geochemistry, Chinese Academy of Sciences, Guiyang, China, ⁵Key Laboratory of Marine Sedimentology and Environmental Geology, First Institute of Oceanography, State Oceanic Administration, Qingdao, China, ⁶State Key Laboratory of Organic Geochemistry, Guangzhou Institute of Geochemistry, Chinese Academy of Sciences, Guangzhou, China

Abstract Black carbon (BC) and polycyclic aromatic hydrocarbons (PAHs) are byproducts generated from the incomplete combustion of organic materials, including fossil fuels and biomass. The similar production processes shared by BC and PAHs provide the possibility to infer the BC sources using the PAHs signatures. This study successfully utilized data sets of BC and PAHs analyzed from the continental shelf surface sediments of the Bohai and Yellow Seas to a standard receptor model of positive matrix factorization (PMF) to apportion the sources of BC in the sediment matrix. Results showed that combustion of fossil fuels (i.e., coal and oil/petroleum) accounted for an average level of $83 \pm 5\%$ of the total BC preserved, which was significantly higher than that from the biomass burning ($17 \pm 5\%$). The spatial distributions of the fossil BC concentrations and percentages differed significantly from those of the biomass BC, implying their different geochemical behaviors in the continental shelf regimes and further emphasizing the importance to effectively differentiate between fossil BC and biomass BC. In addition to the relative proportions of the BC subtypes (char-BC/soot-BC), the regional-specific hydrodynamic conditions, including the cold cyclonic eddy, resuspension and coastal current, also exerted a significant influence on these spatial variations.

1. Introduction

Black carbon (BC), sometimes termed elemental carbon (EC) and pyrogenic carbon (PyC) [Hammes *et al.*, 2007; Wiedemeier *et al.*, 2013, 2015a; Santin *et al.*, 2015], has recently received increasing attention due to its potential importance on regional/global climate change, carbon cycle, air quality, and public health [Fang *et al.*, 2015]. BC is defined as the highly condensed carbonaceous substance released exclusively from the incomplete combustion of organic materials, including biomass and fossil fuels, and it is therefore of purely pyrogenic origin [Hammes *et al.*, 2007]. It has been estimated that the annual global BC formation is 50–260 Tg from biomass burning and 6–24 Tg from fossil fuels combustion, respectively [Mitra *et al.*, 2013]. Due to its widespread production processes and its supposed chemical and microbiological resistance toward degradation, BC becomes an omnipresent component in environmental matrices, such as the atmosphere, soils, fresh/sea water, polar ice/snow, and sediments [Goldberg, 1985]. Of which, marine sediments are usually regarded as the ultimate sink for the terrestrial BC preservation via atmospheric deposition and fluvial input [Mitra *et al.*, 2013].

Though both biomass burning and fossil fuels combustion contribute considerably to the BC emission, and the subsequent transport and burial, BC derived from these two precursors (here defined as biomass BC and fossil BC, respectively) has different physicochemical properties and therefore exhibit different geochemical behaviors in marine regimes, especially in the continental shelf marine systems with large riverine inputs and widely distributed ambient currents [Liu *et al.*, 2007; Hu *et al.*, 2011]. Together with the

recognized dominance of the continental shelf as the major BC sink, which is assumed to account for more than 90% of the global BC burial though the area is only 10% of the world ocean [Suman *et al.*, 1997; Sánchez-García *et al.*, 2012; Mitra *et al.*, 2013; Fang *et al.*, 2015], the distinction and quantification of these two BC source classes in the continental shelf are particularly important. Source apportionment is an effective tool to constrain the relative proportions of biomass BC versus fossil BC. Measurement of radiocarbon isotope of BC is a classical method to apportion the sources of BC in the sediment matrix [Masiello *et al.*, 2002; Reddy *et al.*, 2002; Wang and Li, 2007; Elmquist *et al.*, 2008; Li *et al.*, 2012; Huang *et al.*, 2016]. It has the absolute potential to differentiate between biomass BC and fossil BC, but the high cost of radiocarbon analysis to some extent imposes some restrictions on the application of this method to the large-scale investigations of the sediment BC sources. This implies that one needs to develop an alternative method.

During the incomplete combustion of biomass and fossil fuels, polycyclic aromatic hydrocarbons (PAHs), a group of organic molecular proxies are generated simultaneously [Han *et al.*, 2015]. This means that the molecular signature of PAHs can provide some useful information for the inference of the BC sources [Mitra *et al.*, 2002; Elmquist *et al.*, 2008]. Various techniques, including the biomarkers (e.g., retene, acephenanthrylene, coronene, etc.), isomer pair ratios, principal component analysis (PCA), positive matrix factorization (PMF) model, etc., have been widely used to identify the sources of PAHs [Chen *et al.*, 2011; Lin *et al.*, 2011, 2013; Ma *et al.*, 2014; Wang *et al.*, 2014, 2015]. The PMF model, a receptor model developed originally for analyzing the temporally distributed data sets, has its advantage over others, since it can quantitatively estimate the relative contribution of PAHs from the specific source categories [Lin *et al.*, 2011]. Recently, the PMF model has been successfully applied to the spatially distributed data sets to apportion the sources of PAHs in soils and sediments [Wang *et al.*, 2009; Lin *et al.*, 2011; Ma *et al.*, 2014]. Due to the similar production processes shared by BC and PAHs and the strong association of PAHs with BC during transport [Gustafsson and Gschwend, 1997; Dachs and Eisenreich, 2000], it can be inferred that the application of PMF model merging with PAHs signatures may quantitatively estimate the spatially distributed BC sources. The direct evidence is a study conducted by Hegg *et al.* [2009], who used the spatially distributed data sets of BC and PAHs as well as some other chemical species to the PMF model to apportion the sources of BC in the arctic snow. To the best of our knowledge, however, no attempt has been made to the application of PMF receptor model for the source apportionment of the thermal optical reflectance (TOR) method-based BC in the sediment matrix.

In this study, data sets of BC and PAHs analyzed from the continental shelf surface sediments of the Bohai Sea (BS) and Yellow Sea (YS) [Lin *et al.*, 2011; Fang *et al.*, 2015] were inserted into the PMF receptor model to test its applicability for apportioning the sources of BC in the sediment matrix. Considering that the BS and YS are downwind of the Asian continental outflow in spring and winter when the East-Asian monsoon prevails, and atmospheric deposition has been demonstrated to exert a significant influence on the BC (and also PAHs) inputs into the region [Lang *et al.*, 2008; Lin *et al.*, 2011; Fang *et al.*, 2015], the reasonability of the PMF resolved sediment BC source patterns could then be validated by comparing to the provincial/municipal BC emission inventory and aerosol BC source patterns adjacent to the study area. Based on the validated reliability, the spatial variations of the concentrations and percentages of PMF resolved different combustion-derived BC were further discussed, to reveal their different geochemical behaviors and concurrently identify the possibly associated influential factors. As a whole, the major scientific question of the present study was to apportion the sediment BC sources using PMF receptor model merging with PAHs signatures.

2. Materials and Methods

2.1. Sediment Sampling

The locations of sediment sampling sites in the BS and YS are illustrated in Figure 1. A total of 87 surface sediment samples (0–3 cm) were collected using a stainless steel box corer or grab sampler in two cruises deployed by R/V Dong Fang Hong 2 during 2007–2008. The whole collection of the sediment samples are made up of 35 samples from the BS (B1–B35), 27 samples from the northern YS (NYS) (N1–N27), and 25 samples from the southern YS (SYS) (S1–S25). After collection, they were immediately wrapped in precombusted aluminum foil and stored at -20°C until analysis.

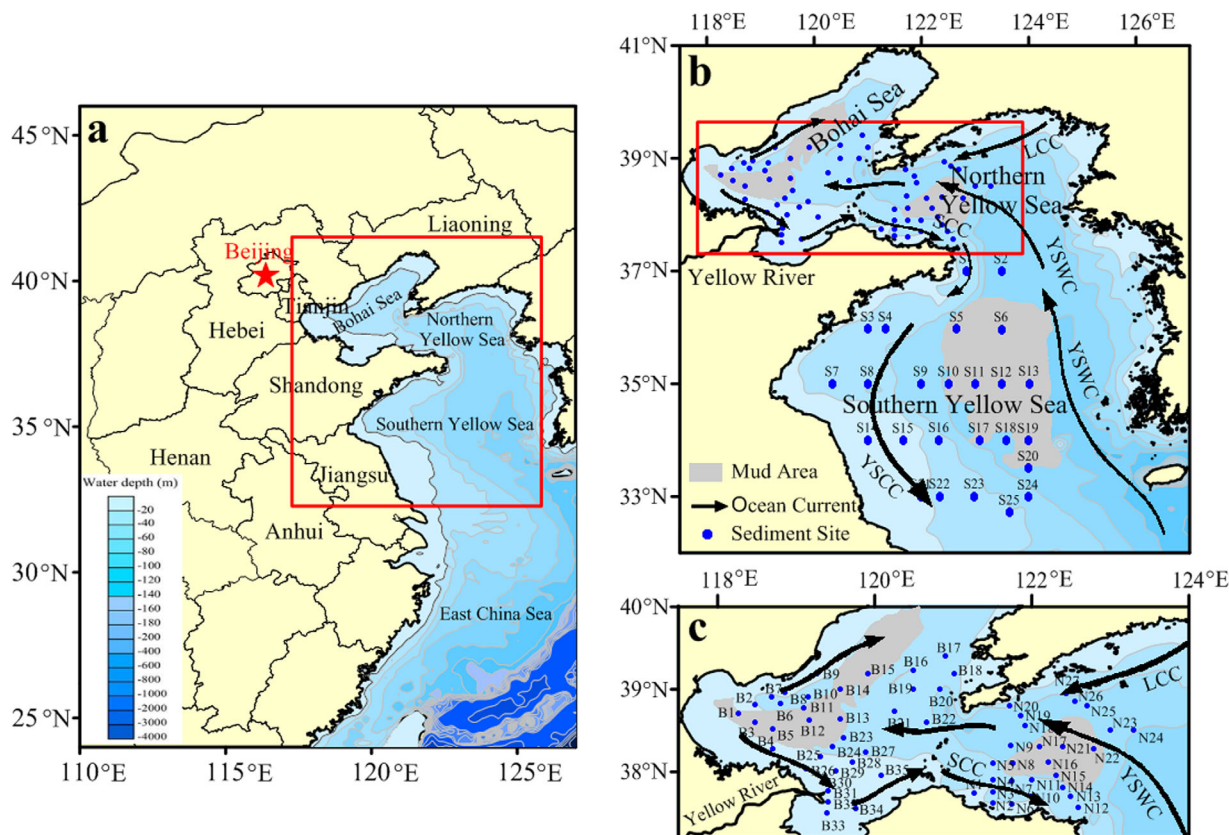


Figure 1. Map showing the (a) study area and (b and c) sediment sampling sites. Circulation systems and mud areas are after Liu *et al.* [2007] and Cheng *et al.* [2004]. YSCC, Yellow Sea Coastal Current; YSWC, Yellow Sea Warm Current; SCC, Shandong Coast Current; LCC, Liaonan Coast Current.

2.2. Analytical Procedures and QA/QC for Sediment BC and PAHs

For sediment BC, various methods have been developed [Hammes *et al.*, 2007; Bird, 2015; Wiedemeier *et al.*, 2015b]. In the present work, the wet-chemical pretreatment combined with thermal optical reflectance (TOR) detection of Han *et al.* [2007] was adopted. Briefly, the thawed, freeze dried, and homogenized (<80 meshes) sediment samples were acids treated to effectively remove the carbonates, silicates, and secondary minerals, and the residues were then filtered through precombusted quartz fiber filters with even distribution. The filters were analyzed for BC on a DRI Model 2001 Thermal/Optical Carbon Analyzer following the IMPROVE_A protocols. Detailed BC analytical procedures are available in our recent work [Fang *et al.*, 2015]. During the sediment BC analysis, blank and replicate samples as well as standard reference material (NIST 1941b) were analyzed simultaneously at a frequency of one per ten samples for QA/QC. The blank samples ($n = 9$) yielded nondetectable BC concentrations, and the relative standard deviation of nine pairs of replicate analyses was in the range of 0–10%, and averaged within 5%. The BC concentration measured in NIST 1941b was 10.45 ± 1.23 mg/g (dry weight, $n = 9$), which was well in accordance with the values reported by recent studies [Han *et al.*, 2007; Cong *et al.*, 2013; Hu *et al.*, 2016], suggesting that the BC analytical method used here was credible and reproducible.

The PAHs analytical procedures followed that described by Mai *et al.* [2003] and Guo *et al.* [2006], and only a brief description is given here. About 10 g of homogenized sediment samples were first spiked with a mixture of recovery surrogate standards of four deuterated PAHs (naphthalene- d_8 , acenaphthene- d_{10} , phenanthrene- d_{10} , and perylene- d_{12}), and then Soxhlet extracted with dichloromethane. The extract was concentrated and fractionated using a silica-alumina (1:1) column. Hexamethylbenzene was added as internal standard and the mixture was reduced and then subjected to GC-MSD analysis (a HP-5972 mass spectrometer interfaced to a HP-5890 II gas chromatography) equipped with a HP-5 capillary column (25 m length \times 0.25 mm id, film thickness 0.25 μ m). The U.S. EPA proposed 16 priority PAHs were the target

compounds measured, including naphthalene (NAP), acenaphthylene (ACY), acenaphthene (ACE), fluorene (FLU), phenanthrene (PHE), anthracene (ANT), fluoranthene (FLUO), pyrene (PYR), benz[a]anthracene (BaA), chrysene (CHR), benzo[b]fluoranthene (BbF), benzo[k]fluoranthene (BkF), benzo[a]pyrene (BaP), indeno[1,2,3-cd]pyrene (INP), dibenz[a,h]anthracene (DBA), and benzo[ghi]perylene (BghiP).

For each batch of 10 sediment samples, a procedural blank, a standard-spiked matrix, a sample duplicate, and a NIST 1941b standard reference material were routinely processed for QA/QC. Procedural blank samples ($n = 9$) contained no detectable amounts of the target analytes. PAHs recoveries of the standard-spiked matrix ranged from 85% to 95%, and the relative percent difference for individual PAHs identified in paired duplicate samples ($n = 9$) was all $< 15\%$. Recoveries of the PAHs in NIST 1941b were between 80% and 120% of the certified values. Limits of detection and quantification (defined as the mean blank value plus 3 and 10 times the standard deviation, respectively) for individual PAH compounds ranged from 0.2 to 2 ng/g and from 0.5 to 3.6 ng/g, respectively. The surrogate standards recoveries were $64.8 \pm 6.8\%$ for naphthalene- d_8 , $67.7 \pm 6.7\%$ for acenaphthene- d_{10} , $97.4 \pm 10.6\%$ for phenanthrene- d_{10} , and $92.7 \pm 17.2\%$ for perylene- d_{12} . The PAHs concentrations here were not recoveries corrected.

2.3. PMF Receptor Model

The strength of PMF receptor model is that it can quantitatively estimate the relative contribution of species from the specific source categories without source profiles, but it requires data sets consisting of a suite of species measured across multiple samples, which is difficult to meet in some cases. Detailed concepts and applications of PMF model for source apportionment were described in EPA PMF 5.0 Fundamentals and User Guide (<http://www.epa.gov/heasd/research/pmf.html>). In principle, the PMF model is based on the following equations:

$$X_{ij} = \sum_{k=1}^p A_{ik} F_{kj} + R_{ij}$$

where X_{ij} is the concentration of the j th congener in the i th sample of the original data sets; A_{ik} is the contribution of the k th factor to the i th sample; F_{kj} is the fraction of the k th factor arising from congener j ; R_{ij} is the residual between the measured X_{ij} and the predicted X_{ij} using p principal components.

$$Q = \sum_{i=1}^n \sum_{j=1}^m \left(\frac{X_{ij} - \sum_{k=1}^p A_{ik} F_{kj}}{S_{ij}} \right)^2$$

where S_{ij} is the uncertainty of the j th congener in the i th sample of the original data sets containing m congeners and n samples. Q is the weighted sum of squares of differences between the PMF output and the original data sets. One of the objectives of PMF analysis is to minimize the Q value.

Before the PMF analysis, both the concentration file and uncertainty file were inserted into the model. In this study, uncertainties of 10% for BC and 20% for PAHs were adopted based on the results from regularly analyzing the replicate samples and the standard reference material (NIST 1941b), respectively [Lin *et al.*, 2011; Fang *et al.*, 2015]. Considering that the concentrations of 27 (31%) samples for ACY, 19 (22%) samples for ACE, and 6 (7%) samples for DBA were below the method detection limit, and the concentrations of these three PAHs compounds in other samples were very low, they were thus not included in the model. Additionally, NAP was also excluded because of the possible evaporative losses during the chemical analysis.

3. Results and Discussion

3.1. Identification of PMF Resolved Factor Profiles

The data sets for PMF analysis here included concentrations and uncertainties for 13 species consisting of 1 BC and 12 selected PAHs from 87 sediment sites collected in the large-scale BS and YS. A critical process in PMF modeling is the determination of the correct number of factors. During the PMF analysis, the model was run for 3–7 factors and was always with random seeds. Finally, the four-factor solution gave the most

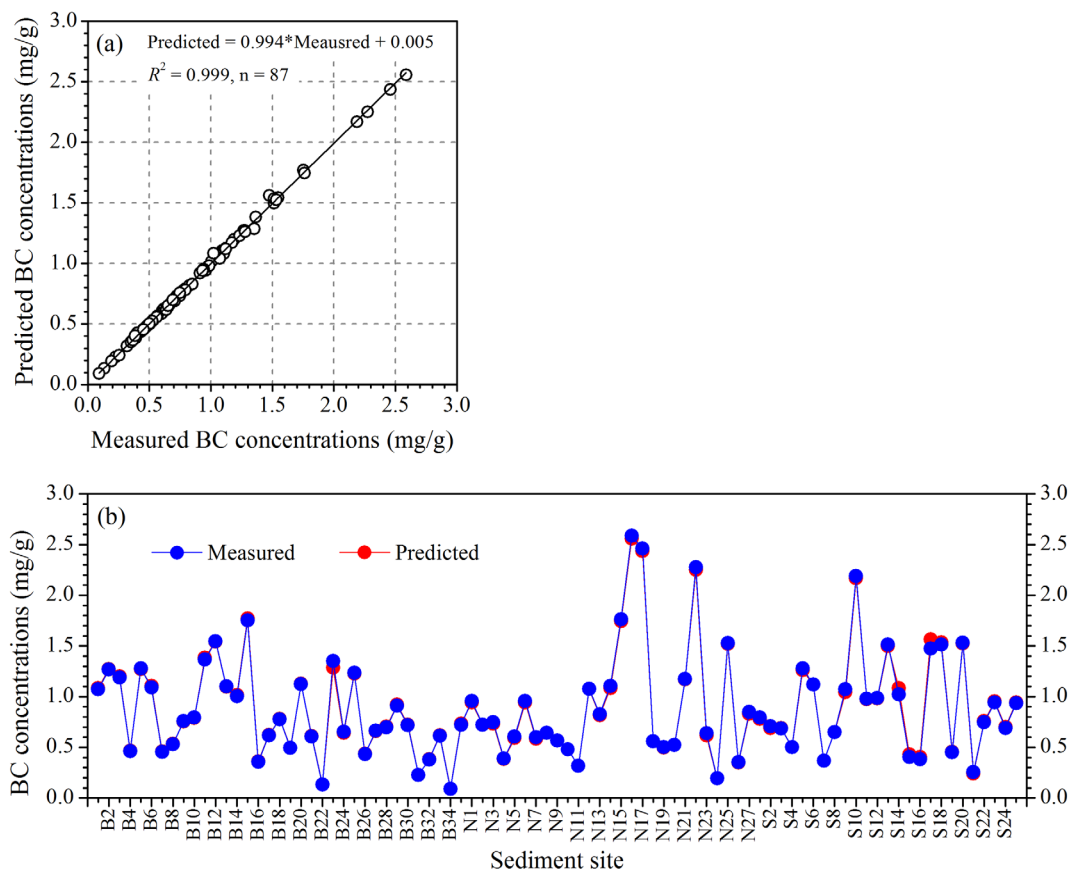


Figure 2. The relationship between the PMF predicted/ modeled BC concentrations and the measured BC concentrations.

stable results and the most easily physically interpretable factors. This solution produced Q values (both robust and true) close to the theoretical Q value, indicating the appropriate uncertainties provided for BC and PAHs data sets in the modeling input. For BC, the species of most concerned, the diagnostic regression R^2 value and the ratio of the PMF predicted concentrations to the measured concentrations were almost unity, and the intercept was nearly zero (Figure 2a). These results suggested that the measured BC concentrations were well modeled by the PMF model (Figure 2b), and they were well explained by the four factors. Diagnostic regression R^2 values for other 12 PAHs were also considerably high, ranging from 0.746 for BaA to 0.981 for BghiP. Taking these facts into consideration, it can be concluded that the four-factor solution was the most meaningful in the light of the BC sources identification. Each factor profile was then identified by comparing to the source profiles from acknowledged references, as illustrated in Figure 3.

Factor 1 was characterized by independently and overwhelmingly high loading of PHE, which was generally believed to be related to crude oil or refined petroleum spill/release and its degradation products [Zakaria *et al.*, 2002]. Moreover, the concentration ratio of ANT/(ANT + PHE) in this factor was less than 0.1, a widely used PAHs source diagnostic ratio indicative of the influence from petroleum residue [Yunker *et al.*, 2002]. Therefore, factor 1 was identified as petroleum residue source. Here petroleum residue represented all uncombusted-petroleum-related activities.

Factor 2 was highly loaded with FLUO, PYR, and PHE, and moderately with BaA, CHR, BbF, and BaP. This factor profile was of high consistency with the PAHs emission characteristics from burning of wood [Bzdusek *et al.*, 2004]. Besides, dominated emissions of FLUO, PYR, and PHE were also observed from burning of crop straws and other vegetation by some researchers [Freeman and Cattell, 1990; Shen *et al.*, 2013]. Consequently, factor 2 was considered as biomass burning.

Profile of factor 3 partly resembled that of factor 2, of which both had high loadings of FLUO, PYR, and PHE. However, there were significant discrepancy existed between them. Compared to factor 2, factor 3 had

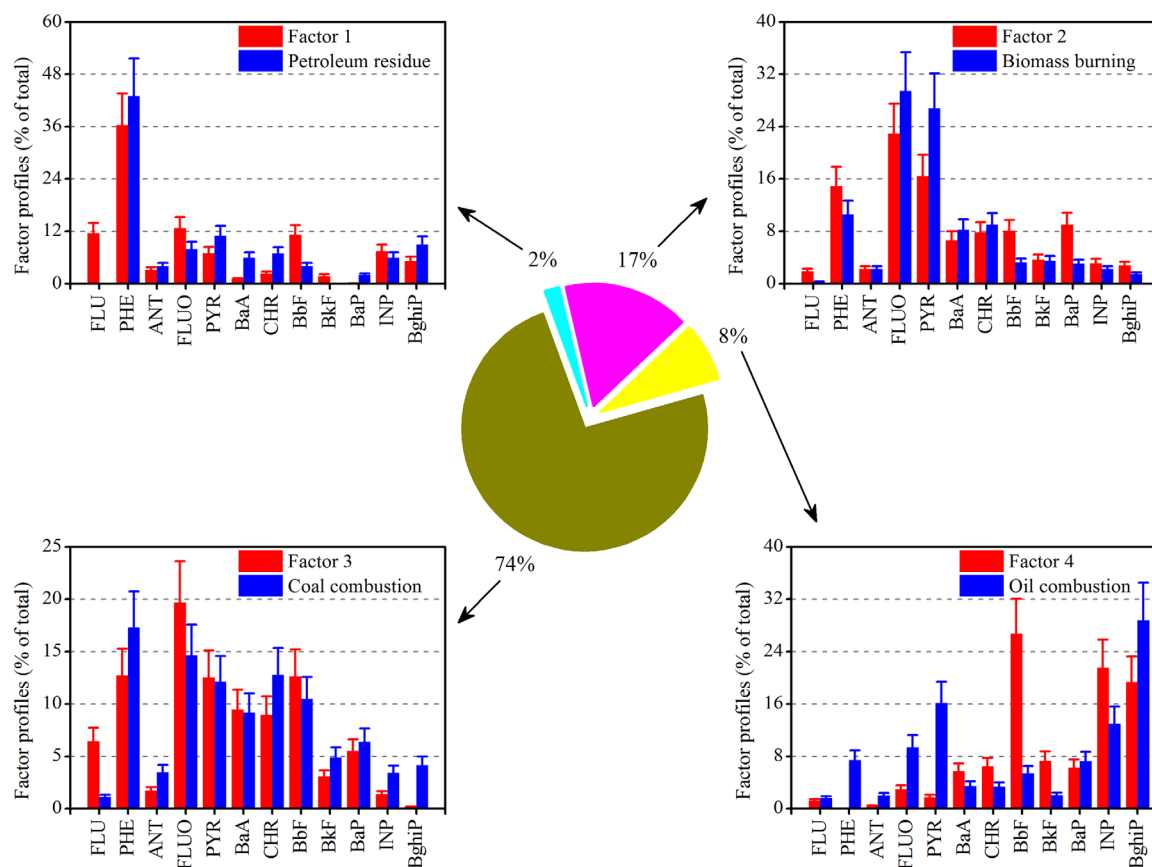


Figure 3. The four-factor profiles resolved from the PMF model and the percentage of each factor contributing to the sediment BC in the entire BS and YS. Source profiles are cited from acknowledged references [Zakaria et al., 2002; Li et al., 2003; Bzdusek et al., 2004; Wang et al., 2009]. Error bars represented a constant relative error of 20%.

higher loadings of moderate molecular weight of four-ring PAHs, including BaA, CHR, and BbF, all of which have been regarded as the organic molecular markers of coal combustion in coke oven, power plants, as well as steel and iron industries [Khalili et al., 1995; Yang et al., 2002; Li et al., 2003]. Thus, factor 3 was selected to represent coal combustion.

Factor 4 was predominantly composed of BbF, INP, and BghiP, and with low loadings of all the remaining PAHs. INP and BghiP were thought to be typical tracers indicative of gasoline and diesel engines emissions [Harrison et al., 1996; Wang et al., 2009], and they were recently suggested to represent this source by numerous studies [Chen et al., 2011; Lin et al., 2011; Ma et al., 2014; Wang et al., 2014, 2015]. Simultaneously, the concentration ratio of INP/(INP + BghiP) in this factor was close to 0.5, also showing a signal of input from the liquid fossil fuel combustion [Yunker et al., 2002]. Hence, factor 4 was assigned as oil combustion process, including the exhausts released from both the inland motor vehicles and sea-going boats/ships.

Though the four factors were identified, it was worth mentioning that there were still some uncertainties associated with the PAHs and therefore BC source identification. In terms of PAHs, in addition to the anthropogenic combustion processes, studies have showed increasing evidences for the biogenic formation in the environment, mainly from the degradation of organic matter [Wilcke, 2007; Wilcke et al., 2014; Nizzetto et al., 2008; Cabrerizo et al., 2011; Guigue et al., 2015]. For instance, PHE, the PAH species with high loadings in factors 1, 2, and 3, can also be produced biologically from alkylphenanthrene precursors in plant debris. Besides, the molecular signals of the PAHs extracted from the sediment receptor might differed from those measured from the nearby emission sources, mainly due to their multiple changes (e.g., aging, selective sorption, etc.) during transport, and the influential parameters altering the PAHs compositions were those pertaining to dry precipitation, surface-to-air diffusion, degradation in air and water, and exchange between water and sediment [Zhang et al., 2005]. In terms of BC, the TOR method might produce some false positive

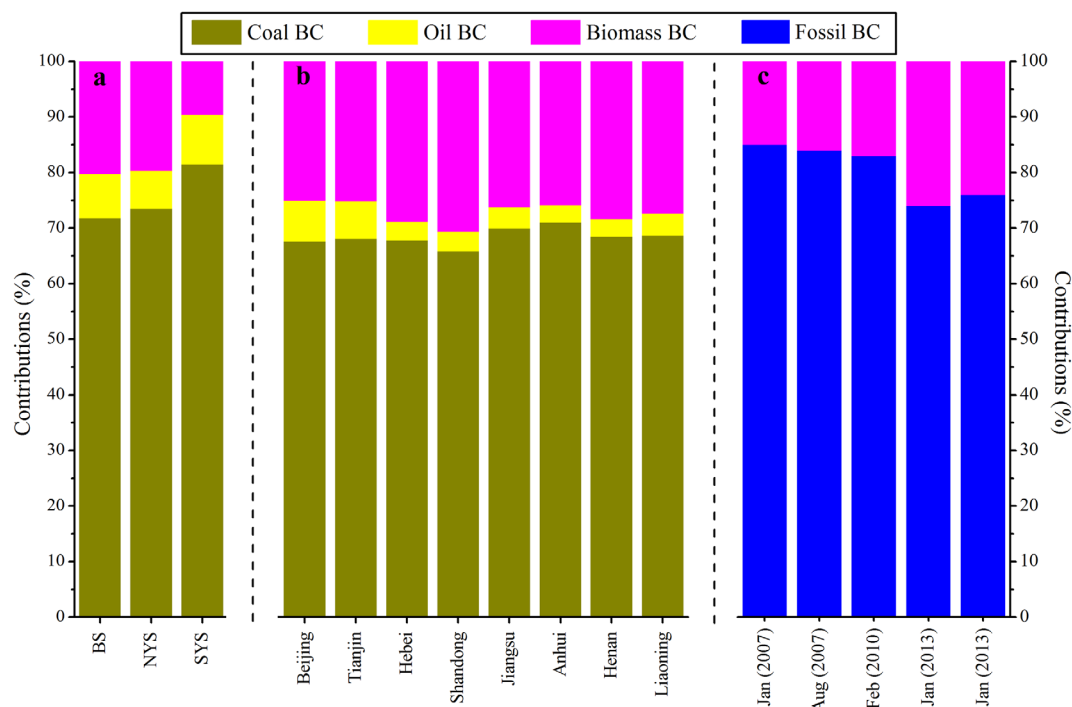


Figure 4. Comparisons between (a) the sediment BC source patterns in the BS, NYS, and SYS subregions, and (b) the provincial/municipal BC emission inventory adjacent to the BS and YS [Cao *et al.*, 2006] and (c) radiocarbon-based aerosol BC source patterns in the municipality of Beijing, the capital of China (including three different months during 2007–2013) [Sun *et al.*, 2012; Chen *et al.*, 2013; Andersson *et al.*, 2015; Zhang *et al.*, 2015b].

[Hammes *et al.*, 2007]. Unfortunately, however, we could not quantitatively estimate the impacts of these factors on the sediment BC source apportionment.

The loading of BC concentration in factor of petroleum residue was significantly (4–38 times) lower than that in the other three factors, implying the negligible contribution ($\sim 2\%$) of BC from petroleum residue (Figure 3), which coincided well with the fact that BC was of purely pyrogenic origin. Because of this, we can make some simplifications by deducting the negligible petroleum residue source and then normalizing the remaining three combustion sources to 100%. These simplifications were conducive for the following validation of the PMF resolved sediment BC source patterns by comparing to the BC emission inventory and aerosol BC source patterns, both of which were based on the pure combustion sources.

3.2. PMF Resolved Sediment BC Source Patterns in the BS and YS and Their Validations

The PMF resolved sediment BC source patterns in the BS, NYS, and SYS are shown in Figure 4a. Overall, the BS and NYS had the similar sediment BC source patterns, with the highest contribution from coal combustion, followed by biomass burning and oil combustion. The BC source patterns of the SYS differed slightly from that of the BS and NYS, which exhibited a relatively higher contribution from coal combustion but a lower contribution from biomass burning. Specifically, coal combustion, oil combustion, and biomass burning each contributed to $\sim 72\%$, $\sim 8\%$, and $\sim 20\%$ of the total sediment BC for BS, and they were $\sim 73\%$, $\sim 7\%$, and $\sim 20\%$ for NYS and $\sim 81\%$, $\sim 9\%$, and $\sim 10\%$ for SYS. Taking the coal combustion and oil combustion together, it can be obtained that the fossil BC in the BS and YS accounted for 80–90% (average, $83 \pm 5\%$) of the sediment BC sources, significantly higher than the biomass BC source, which only contributed to 10–20% (average, $17 \pm 5\%$).

Due to a combination of the importance of atmospheric deposition on the delivery of BC (and also of PAHs) to the BS and YS (atmospheric deposition accounted for more than 50% of the total BC input) [Lang *et al.*, 2008; Lin *et al.*, 2011; Fang *et al.*, 2015], and the negligible degradation of BC occurred in the 0–3 cm surface sediments (representing particles deposited by recent several years to few decades), it is therefore meaningful to make comparisons between the sediment BC source patterns and the adjacent provincial/

Table 1. Reported BC Sources in the Continental Shelf Surface Sediments

Locations	Descriptions	BC Contributions (%)		Method Used	References
		Fossil Fuels	Biomass		
Bohai and Yellow Seas	Large-scale continental shelf, surface 0–3 cm, sampled in 2007–2008	80–90	10–20	PMF modeling using BC and PAHs as input data	This study
Yangtze River Estuary	Sampling sites are largely affected by Yangtze River input, surface 0–10 cm, sampled in 2003	60–80	20–40	Radiocarbon isotope (¹⁴ C)	Wang and Li [2007]
Yangtze River Estuary	Sampling sites are largely affected by Yangtze River input, surface 0–1 cm, sampled in 2009–2010	46–48	52–54	Radiocarbon isotope (¹⁴ C)	Li et al. [2012]
Yangtze River Estuary	Sampling sites are largely affected by Yangtze River input, surface 0–1 cm, sampled in 2006–2011	52–71	29–48	Radiocarbon isotope (¹⁴ C)	Huang et al. [2015]
Pearl River Estuary	Sampling sites are largely affected by Pearl River input, surface 0–5 cm, sampled in 2000	65–80	20–35	Stable carbon isotope (¹³ C)	Sun et al. [2008]
Chesapeake Bay, USA	Fossil inputs (especially vehicular and industrial emissions) dominate, surface 0–10 cm, sampled in 1991	~90	~10	Radiocarbon isotope (¹⁴ C)	Reddy et al. [2002]
New York Bay and Newark Bay, USA	Fossil inputs (especially vehicular and industrial emissions) dominate, surface 0–10 cm, sampled in 1994	~90	~10	Radiocarbon isotope (¹⁴ C)	Reddy et al. [2002]
Pan-Arctic Estuary	Surface 0–2 cm, sampled in 2004–2005	12–95	5–88	Radiocarbon isotope (¹⁴ C)	Elmqvist et al. [2008]

municipal BC emission inventory and aerosol BC source patterns, which may provide some insights into the validation of the PMF resolved sediment BC source patterns.

The provincial/municipal BC emission inventory adjacent to the BS and YS including that in Beijing, Tianjin, Hebei, Shandong, Jiangsu, Anhui, Henan, and Liaoning (Figure 1a) is presented in Figure 4b. Apparently, coal combustion was the dominant contributor to the total BC emission in these areas, which accounted for a comparable fraction of $68 \pm 1\%$ to that in the sediment BC sources ($75 \pm 4\%$). The consistency of the dominant contributions from coal combustion between the sediment BC source patterns and the BC emission inventory to some extent validated the reliability of the PMF modeling output. Despite this similarity, some differences did occur. In terms of the BC emission inventory, oil combustion accounted for $4 \pm 2\%$ of the total BC emission, which was only one half to that of the sediment BC ($8 \pm 1\%$). As we know, the BS and YS are important bases of fishery and port [Zhang et al., 2014], and large quantities of fishing boats and merchant ships are traveling constantly on these sea areas. Taking small fishing boats as an example, there were 1.07 million in China by the end of 2013 (Chinese Fishery Statistical Yearbook, 2014). They basically had no particulate matter emission control measures. It was expected that a significant amount of BC was emitted from these boats [Zhang et al., 2014, 2015a], which inevitably contributed to the oil combustion-derived BC (here defined as oil BC) in the sediments. However, BC emissions from the seagoing boats/ships were not included in the current BC emission inventory [Cao et al., 2006], resulting in a relatively higher fraction of oil BC in the sediment than that in the emission inventory. The resultant was the lower biomass BC in the sediments ($17 \pm 5\%$) than that in the emission inventory ($27 \pm 2\%$). The discrepancy of oil BC between sediments and emission inventory implied that future BC emission inventory development should pay more attention to the BC emissions from seagoing boats/ships, which not only contribute to the sediment BC burial/sequestration, but more importantly also exert a significant influence on the ambient air quality of coastal cities with densely distributed populations [Zhang et al., 2014, 2015a].

In recent years, there are several radiocarbon-based source apportionment studies of aerosol BC conducted in the municipality of Beijing, the capital of China (Figure 1a). Results showed that $80 \pm 4\%$ of the aerosol BC was attributed to the combustion of fossil fuels, with the remaining $20 \pm 4\%$ from the biomass burning (Figure 4c). The PMF resolved sediment BC sources were highly consistent with the adjacent aerosol BC source patterns, again validating the reliability of the PMF modeling output. Based on the above cross comparisons and discussions, it can be concluded that the PMF receptor model merging with PAHs signatures was successfully applied to apportion the sources of BC in the sediment matrix.

Table 1 lists the sediment BC sources conducted in the continental shelf regimes. In contrast to the large-scale investigations in the present study, which reflected the regional BC source patterns, the sampling campaign conducted in the large river influenced estuary regions reflected the local BC source patterns, and had relatively lower proportions of fossil BC and the correspondingly higher fractions of biomass BC. For instance, fossil (biomass) BC contributed to 46–80% (20–54%) and 65–80% (20–35%) of the total BC deposited in the Yangtze River estuary and the Pearl River estuary, respectively [Wang and Li, 2007; Sun

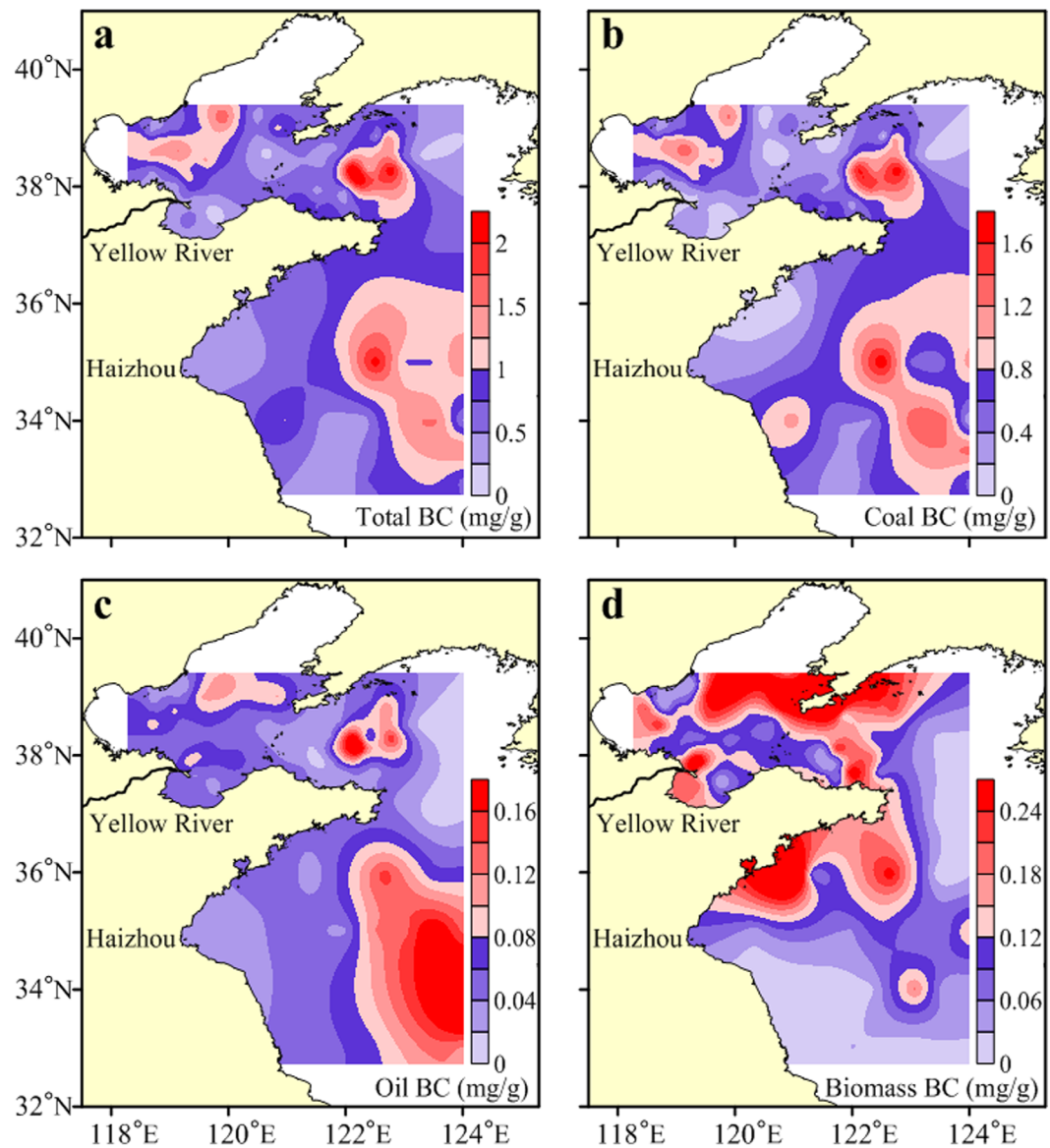


Figure 5. The spatial distributions of the concentrations of the (a) total BC and (b–d) PMF resolved coal BC, oil BC, and biomass BC.

et al., 2008; *Li et al.*, 2012; *Huang et al.*, 2016]. This difference might be associated with the influence from riverine discharge, which increased the delivery of the larger-sized biomass BC and conversely declined the fraction of the smaller-sized fossil BC (see section 3.3). In addition, radiocarbon-based assessment found that sediments in seven pan-Arctic estuaries showed a wider range of fossil (biomass) BC input, ranging from ~12% (~88%) in the Yenisey River estuary to ~95% (~5%) in the Lena River estuary [*Elmqvist et al.*, 2008]. Therefore, the sources of BC in the continental shelf surface sediments differed significantly among regions, implying that a global-scale investigation of the sediment BC sources would be of great importance. The application of PMF receptor model merging with PAHs signatures like in the present study may be an alternative method for addressing this issue.

3.3. Spatial Variations of Fossil BC Versus Biomass BC: Influence of BC Subtypes and Hydrodynamic Conditions

The spatial distributions of the total BC and PMF resolved fossil BC (including coal BC and oil BC) and biomass BC concentrations are figured in Figure 5. Apparently, the spatial distribution of the coal BC resembled that of the total BC, with high concentrations mainly occurring in the central parts of the BS, NYS, and SYS,

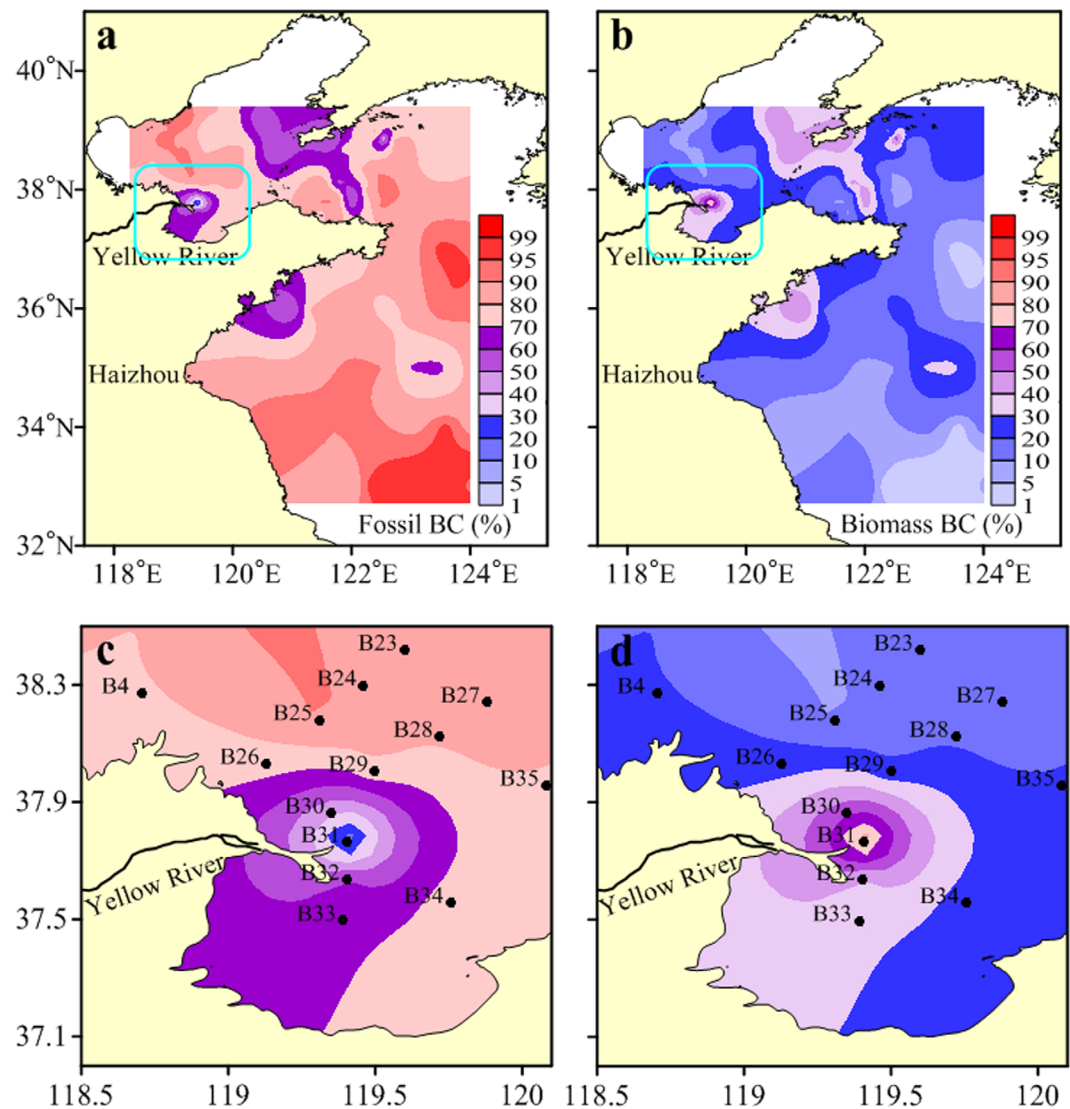


Figure 6. The spatial distributions of the percentages of the (a, c) fossil BC and (b, d) biomass BC.

and with low values in the eastern BS, the eastern NYS, the Haizhou Bay, and the southwestern SYS. The coal BC constituted a vast majority of the total BC (>70%), the consistent distributions between the coal BC and the total BC were thus not surprising. For the oil BC, which accounted for only ~8% of the total BC, also exhibited a similar pattern to that of the total BC and therefore the coal BC, suggesting that these two types of fossil BC might have the similar production mechanisms and/or transport pathways. However, the distribution of the biomass BC differed significantly from that of the total BC and the fossil BC, with high values occurring in the nearshore areas and low values in the central parts, which indicated the different geochemical behaviors between the biomass BC and fossil BC in these continental shelf regimes. The current BC concentrations patterns resulted in a seaward increasing trend for the percentage of the fossil BC and a correspondingly seaward decreasing trend for the percentage of the biomass BC (Figure 6).

BC is not a well-defined component, but rather exists as a combustion/temperature continuum [Masiello, 2004]. Scientists often classify BC into two subtypes, i.e., char-BC and soot-BC [Hammes *et al.*, 2007; Han *et al.*, 2015; Hu *et al.*, 2016]. Although fossil fuels combustion and biomass burning both produce BC, the relative proportions of the char-BC and soot-BC (char-BC/soot-BC) varies as a function of the fuel types and other factors. Generally, biomass burning with low temperatures generates a higher ratio of char-BC/soot-BC than that of the fossil fuels combustion [Han *et al.*, 2015]. Compared to the char-BC, which is the partly burned residue of original, often solid fuel phase and is within 1–100 μm , the soot-BC formed through

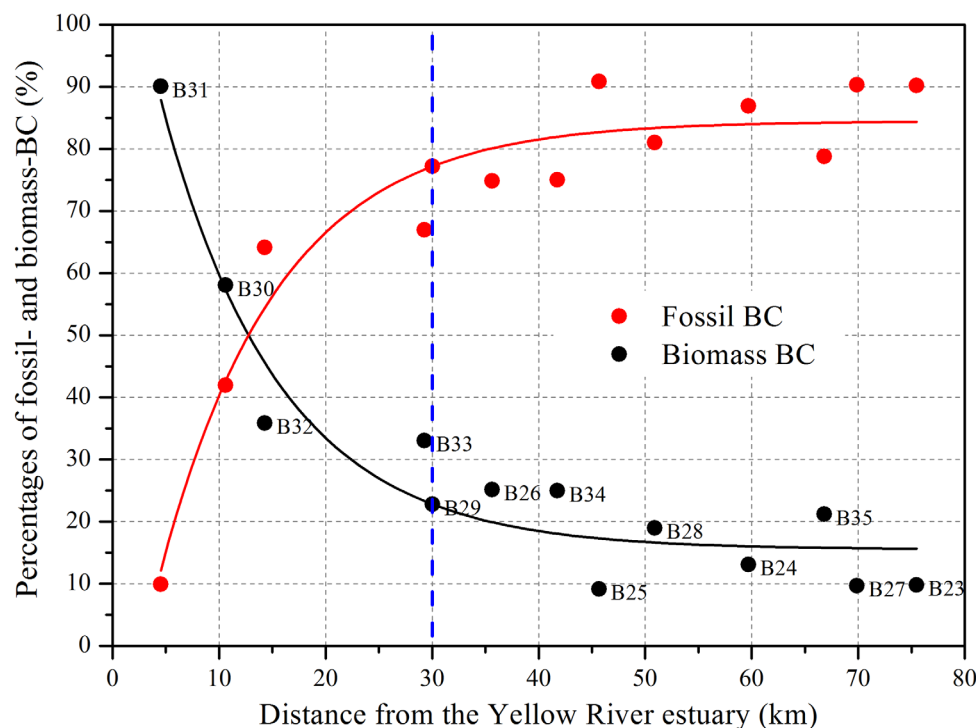


Figure 7. Percentages of the fossil BC and biomass BC versus the distance from the Yellow River estuary.

assembly of gas-phase precursors is much smaller (less than $1 \mu\text{m}$) [Elmqvist *et al.*, 2008]. This implied that the more soot-BC contained fossil BC was more prone to subject to long-range atmospheric and water transport than that of the biomass BC, which might explain the above seaward increasing trend for the fossil BC and the conversely seaward decreasing trend for the biomass BC. Here of particular notable was the convergence effect of the cold cyclonic eddy occurring in the central areas of the NYS and SYS. Such effect might be more pronounced in affecting the transport and subsequent deposition/sequestration of the smaller-sized fossil BC, resulting in the highest fossil BC concentrations and percentages in these central areas.

Despite the above holistic trends, the increasing and decreasing rates varied among different areas. The highest varying rates took place in the Yellow River estuary, as clearly indicated by the sharply changed colors (Figures 6c and 6d). Within ~ 5 – 30 km away from the Yellow River estuary, the percentage of the fossil BC increased exponentially from $\sim 10\%$ to $\sim 80\%$, and that of the biomass BC declined exponentially from $\sim 90\%$ to $\sim 20\%$ (Figure 7). This dramatic variation might be related to the regional-specific hydrodynamic conditions. It is estimated that more than 80% of the Yellow River-derived sediments discharges into the BS during the summertime [Bi *et al.*, 2011]. During this period, the water column is highly stratified and the vertical mixing is markedly weakened, leading to the rapid deposition of these river-derived sediments within ~ 30 km of the Yellow River estuary. During the winter, however, the strong northerly and north-westerly East-Asian monsoon prevails, and it generates waves up to ~ 7 m that propagate toward the coast of the Yellow River delta [Bi *et al.*, 2011]. The large waves bring about the intensive resuspension of the estuary seabed sediments off the Yellow River delta due to the elevated bottom shear stress [Yang *et al.*, 2011]. Moreover, the intense vertical mixing maintains the sediments in suspension. These conditions together with the easterly coastal current (Figure 1b) are conducive for the sediments and their associated BC particles transport outward. Because of the easier transportability of the fossil BC compared to that of the biomass BC, the percentage of the fossil BC would increase seaward, and the resultant was the declined percentage of the biomass BC. The direct manifestation might be the here observed seaward exponentially increasing trend for the fossil BC and the exponentially decreasing trend for the biomass BC (Figure 7). Beyond ~ 30 km away from the Yellow River estuary, however, the percentages of the fossil BC and biomass BC changed slightly due to the significantly weakened hydrodynamic conditions.

To conclude, the spatial variations of the fossil BC and biomass BC to a large extent attributed to their relative proportions of BC subtypes (char-BC/soot-BC) and the regional-specific hydrodynamic conditions, including the cold cyclonic eddy, resuspension, and coastal current.

4. Conclusions

In this study, data sets of BC and PAHs analyzed from the continental shelf surface sediments of the BS and YS were inserted into the PMF receptor model to apportion the sources of BC in the sediment matrix. Four factors (i.e., petroleum residue, coal combustion, oil combustion, and biomass burning) were identified, but BC from factor of petroleum residue was negligible, which was a reasonable result. Combustion of fossil fuels was the dominant BC source, accounting for an average level of $83 \pm 5\%$, significantly higher than that from the biomass burning ($17 \pm 5\%$). Cross comparisons between the sediment BC source patterns and the provincial/municipal BC emission inventory and aerosol BC source patterns adjacent to the BS and YS validated the reliability of the PMF resolved sediment BC source patterns. The spatial distributions of the concentrations and percentages of fossil BC differed significantly from those of biomass BC, exhibiting the increasing seaward trend for the fossil BC and decreasing seaward trend for the biomass BC, suggesting that the fossil BC and biomass BC had different geochemical behaviors in these continental shelf regimes. More pronounced varying rates of the percentages of the fossil BC and biomass BC occurred within $\sim 5\text{--}30$ km away from the Yellow River estuary. The spatial variations between the fossil BC and biomass BC were mainly attributed to their relative proportions of BC subtypes (char-BC/soot-BC) and the regional-specific hydrodynamic conditions. These findings emphasized the importance to effectively differentiate between fossil BC and biomass BC in future sediment BC studies. The application of PMF receptor model merging with PAHs signatures may be an alternative method, but it is only suitable for the large-scale investigations due to its inherent demand of data volume.

Acknowledgments

This work was financially supported by the Strategic Priority Research Program of the Chinese Academy of Sciences (CAS) (XDA11020402 and XDB05030303), the Knowledge Innovation Program of the CAS (KZCX2-YW-QN210), and the National Natural Scientific Foundation of China (41473091, 41273135, 41073064, and 41206055). The authors are most grateful to the crew of R/V *Dong Fang Hong 2* of Ocean University of China for collecting the sediment samples. We also thank two anonymous reviewers who provided constructive comments which strengthened the manuscript. Please contact the corresponding author at yjchentj@tongji.edu.cn to obtain the data used in this paper.

References

- Andersson, A., J. J. Deng, K. Du, M. Zheng, C. Q. Yan, M. Skold, and Ö. Gustafsson (2015), Regionally-varying combustion sources of the January 2013 severe haze events over Eastern China, *Environ. Sci. Technol.*, *49*(4), 2038–2043, doi:10.1021/es503855e.
- Bi, N. S., Z. S. Yang, H. J. Wang, D. J. Fan, X. X. Sun, and K. Lei (2011), Seasonal variation of suspended-sediment transport through the southern Bohai Strait, *Estuarine Coastal Shelf Sci.*, *93*(3), 239–247, doi:10.1016/j.ecss.2011.03.007.
- Bird, M. I. (2015), Test procedures for biochar analysis in soils, in *Biochar for Environmental Management: Science, Technology and Implementation*, edited by J. Lehmann and S. Joseph, pp. 679–716, Earthscan, London, U. K.
- Bzdusek, P. A., E. R. Christensen, A. Li, and Q. M. Zou (2004), Source apportionment of sediment PAHs in Lake Calumet, Chicago: Application of factor analysis with nonnegative constraints, *Environ. Sci. Technol.*, *38*(1), 97–103, doi:10.1021/es034842k.
- Cabrero, A., J. Dachs, C. Moeckel, M.-J. Ojeda, G. Caballero, D. Barcelo, and K. C. Jones (2011), Ubiquitous net volatilization of polycyclic aromatic hydrocarbons from soils and parameters influencing their soil-air partitioning, *Environ. Sci. Technol.*, *45*(11), 4740–4747, doi:10.1021/es104131f.
- Cao, G. L., X. Y. Zhang, and F. C. Zheng (2006), Inventory of black carbon and organic carbon emissions from China, *Atmos. Environ.*, *40*(34), 6516–6527, doi:10.1016/j.atmosenv.2006.05.070.
- Chen, B., et al. (2013), Source forensics of black carbon aerosols from China, *Environ. Sci. Technol.*, *47*(16), 9102–9108, doi:10.1021/es401599r.
- Chen, Y. J., Y. L. Feng, S. C. Xiong, D. Y. Liu, G. Wang, G. Y. Sheng, and J. M. Fu (2011), Polycyclic aromatic hydrocarbons in the atmosphere of Shanghai, China, *Environ. Monit. Assess.*, *172*(1–4), 235–247, doi:10.1007/s10661-010-1330-x.
- Cheng, P., S. Gao, and H. Bokuniewicz (2004), Net sediment transport patterns over the Bohai Strait based on grain size trend analysis, *Estuarine Coastal Shelf Sci.*, *60*(2), 203–212, doi:10.1016/j.ecss.2003.12.009.
- Cong, Z. Y., S. C. Kang, S. P. Gao, Y. L. Zhang, Q. Li, and K. Kawamura (2013), Historical trends of atmospheric black carbon on Tibetan Plateau as reconstructed from a 150-year lake sediment record, *Environ. Sci. Technol.*, *47*(6), 2579–2586, doi:10.1021/es3048202.
- Dachs, J., and S. J. Eisenreich (2000), Adsorption onto aerosol soot carbon dominates gas-particle partitioning of polycyclic aromatic hydrocarbons, *Environ. Sci. Technol.*, *34*(17), 3690–3697, doi:10.1021/es991201+.
- Elmqvist, M., I. Semiletov, L. D. Guo, and Ö. Gustafsson (2008), Pan-Arctic patterns in black carbon sources and fluvial discharges deduced from radiocarbon and PAH source apportionment markers in estuarine surface sediments, *Global Biogeochem. Cycles*, *22*, GB2018, doi:10.1029/2007GB002994.
- Fang, Y., Y. J. Chen, C. G. Tian, T. Lin, L. M. Hu, G. P. Huang, J. H. Tang, J. Li, and G. Zhang (2015), Flux and budget of BC in the continental shelf seas adjacent to Chinese high BC emission source regions, *Global Biogeochem. Cycles*, *29*, 957–972, doi:10.1002/2014GB004985.
- Freeman, D. J., and F. C. R. Cattell (1990), Woodburning as a source of atmospheric polycyclic aromatic hydrocarbons, *Environ. Sci. Technol.*, *24*(10), 1581–1585, doi:10.1021/es00080a019.
- Goldberg, E. D. (1985), *Black Carbon in the Environment*, John Wiley, N. Y.
- Guigue, C., L. Bigot, J. Turquet, M. Tedetti, N. Ferretto, M. Goutx, and P. Cuet (2015), Hydrocarbons in a coral reef ecosystem subjected to anthropogenic pressures (La Reunion Island, Indian Ocean), *Environ. Chem.*, *12*(3), 350–365, doi:10.1071/EN14194.
- Guo, Z. G., T. Lin, G. Zhang, Z. S. Yang, and M. Fang (2006), High-resolution depositional records of polycyclic aromatic hydrocarbons in the Central Continental Shelf Mud of the East China Sea, *Environ. Sci. Technol.*, *40*(17), 5304–5311, doi:10.1021/es060878b.
- Gustafsson, Ö., and P. M. Gschwend (1997), Soot as a strong partition medium for polycyclic aromatic hydrocarbons in aquatic systems, in *Molecular Markers in Environmental Geochemistry*, edited by R. P. Eganhouse, pp. 365–381, Am. Chem. Soc., Washington, D. C.

- Hammes, K., et al. (2007), Comparison of quantification methods to measure fire-derived (black/elemental) carbon in soils and sediments using reference materials from soil, water, sediment and the atmosphere, *Global Biogeochem. Cycles*, *21*, GB3016, doi:10.1029/2006GB002914.
- Han, Y. M., J. J. Cao, Z. S. An, J. C. Chow, J. G. Watson, Z. D. Jin, K. Fung, and S. X. Liu (2007), Evaluation of the thermal/optical reflectance method for quantification of elemental carbon in sediments, *Chemosphere*, *69*(4), 526–533, doi:10.1016/j.chemosphere.2007.03.035.
- Han, Y. M., et al. (2015), Elemental carbon and polycyclic aromatic compounds in a 150-year sediment core from Lake Qinghai, Tibetan Plateau, China: Influence of regional and local sources and transport pathways, *Environ. Sci. Technol.*, *49*(7), 4176–4183, doi:10.1021/es504568m.
- Harrison, R. M., D. J. T. Smith, and L. Luhana (1996), Source apportionment of atmospheric polycyclic aromatic hydrocarbons collected from an urban location in Birmingham, UK, *Environ. Sci. Technol.*, *30*(3), 825–832, doi:10.1021/es950252d.
- Hegg, D. A., S. G. Warren, T. C. Grenfell, S. J. Doherty, T. V. Larson, and A. D. Clarke (2009), Source attribution of black carbon in arctic snow, *Environ. Sci. Technol.*, *43*(11), 4016–4021, doi:10.1021/es803623f.
- Hu, L. M., T. Lin, X. F. Shi, Z. S. Yang, H. J. Wang, G. Zhang, and Z. G. Guo (2011), The role of shelf mud depositional process and large river inputs on the fate of organochlorine pesticides in sediments of the Yellow and East China seas, *Geophys. Res. Lett.*, *38*, L03602, doi:10.1029/2010GL045723.
- Hu, L. M., X. F. Shi, Y. Z. Bai, Y. Fang, Y. J. Chen, S. Q. Qiao, S. F. Liu, G. Yang, N. Kornkanitnan, and S. Khokiattiwong (2016), Distribution, input pathway and mass inventory of black carbon in sediments of the Gulf of Thailand, SE Asia, *Estuarine Coastal Shelf Sci.*, *170*, 10–19, doi:10.1016/j.ecss.2015.12.019.
- Huang, L., J. Zhang, Y. Wu, and J. L. Wang (2016), Distribution and preservation of black carbon in the East China Sea sediments: Perspectives on carbon cycling at continental margins, *Deep Sea Res., Part II*, *124*, 43–52, doi:10.1016/j.dsr2.2015.04.029.
- Khalili, N. R., P. A. Scheff, and T. M. Holsen (1995), PAH source fingerprints for coke ovens, diesel and gasoline engines, highway tunnels, and wood combustion emissions, *Atmos. Environ.*, *29*(4), 533–542, doi:10.1016/1352-2310(94)00275-P.
- Lang, C., S. Tao, W. X. Liu, Y. X. Zhang, and S. Simonich (2008), Atmospheric transport and outflow of polycyclic aromatic hydrocarbons from China, *Environ. Sci. Technol.*, *42*(14), 5196–5201, doi:10.1021/es800453n.
- Li, A., J.-K. Jang, and P. A. Scheff (2003), Application of EPA CMB8.2 model for source apportionment of sediment PAHs in Lake Calumet, Chicago, *Environ. Sci. Technol.*, *37*(13), 2958–2965, doi:10.1021/es026309v.
- Li, X. X., T. S. Bianchi, M. A. Allison, P. Chapman, S. Mitra, Z. R. Zhang, G. P. Yang, and Z. G. Yu (2012), Composition, abundance and age of total organic carbon in surface sediments from the inner shelf of the East China Sea, *Mar. Chem.*, *145–147*, 37–52, doi:10.1016/j.marchem.2012.10.001.
- Lin, T., L. M. Hu, Z. G. Guo, Y. W. Qin, Z. S. Yang, G. Zhang, and M. Zheng (2011), Sources of polycyclic aromatic hydrocarbons to sediments of the Bohai and Yellow Seas in East Asia, *J. Geophys. Res.*, *116*, D23305, doi:10.1029/2011JD015722.
- Lin, T., L. M. Hu, Z. G. Guo, G. Zhang, and Z. S. Yang (2013), Deposition fluxes and fate of polycyclic aromatic hydrocarbons in the Yangtze River estuarine-inner shelf in the East China Sea, *Global Biogeochem. Cycles*, *27*, 77–87, doi:10.1029/2012GB004317.
- Liu, J. P., K. H. Xu, A. C. Li, J. D. Milliman, D. M. Velozzi, S. B. Xiao, and Z. S. Yang (2007), Flux and fate of Yangtze River sediment delivered to the East China Sea, *Geomorphology*, *85*(3–4), 208–224, doi:10.1016/j.geomorph.2006.03.023.
- Ma, C. L., S. Y. Ye, T. Lin, X. G. Ding, H. M. Yuan, and Z. G. Guo (2014), Source apportionment of polycyclic aromatic hydrocarbons in soils of wetlands in the Liao River Delta, Northeast China, *Mar. Pollut. Bull.*, *80*(1–2), 160–167, doi:10.1016/j.marpolbul.2014.01.019.
- Mai, B. X., S. H. Qi, E. Y. Zeng, Q. S. Yang, G. Zhang, J. M. Fu, G. Y. Sheng, P. A. Peng, and Z. S. Wang (2003), Distribution of polycyclic aromatic hydrocarbons in the Coastal Region off Macao, China: Assessment of input sources and transport pathways using compositional analysis, *Environ. Sci. Technol.*, *37*(21), 4855–4863, doi:10.1021/es034514k.
- Masiello, C. A. (2004), New directions in black carbon organic geochemistry, *Mar. Chem.*, *92*(1–4), 201–213, doi:10.1016/j.marchem.2004.06.043.
- Masiello, C. A., E. R. M. Druffel, and L. A. Currie (2002), Radiocarbon measurements of black carbon in aerosols and ocean sediments, *Geochim. Cosmochim. Acta*, *66*(6), 1025–1036, doi:10.1016/S0016-7037(01)00831-6.
- Mitra, S., T. S. Bianchi, B. A. McKee, and M. Sutula (2002), Black carbon from the Mississippi River: Quantities, sources, and potential implications for the global carbon cycle, *Environ. Sci. Technol.*, *36*(11), 2296–2302, doi:10.1021/es015834b.
- Mitra, S., A. R. Zimmerman, G. Hunsinger, and W. R. Woerner (2013), Black carbon in coastal and large river systems, in *Biogeochemical Dynamics at Major River-Coastal Interfaces: Linkages With Global Change*, edited by T. Bianchi, M. Allison, and W. J. Cai, pp. 200–234, Cambridge Univ. Press, N. Y.
- Nizzetto, L., R. Lohmann, R. Gioia, A. Jahnke, C. Temme, J. Dachs, P. Herckes, A. Di Guardo, and K. C. Jones (2008), PAHs in air and seawater along a North-South Atlantic transect: Trends, processes and possible sources, *Environ. Sci. Technol.*, *42*(5), 1580–1585, doi:10.1021/es0717414.
- Reddy, C. M., A. Pearson, L. Xu, A. P. McNichol, B. A. Benner Jr., S. A. Wise, G. A. Klouda, L. A. Currie, and T. I. Eglinton (2002), Radiocarbon as a tool to apportion the sources of polycyclic aromatic hydrocarbons and black carbon in environmental samples, *Environ. Sci. Technol.*, *36*(8), 1774–1782, doi:10.1021/es011343f.
- Sánchez-García, L., I. Cato, and Ö. Gustafsson (2012), The sequestration sink of soot black carbon in the Northern European Shelf sediments, *Global Biogeochem. Cycles*, *26*, GB1001, doi:10.1029/2010GB003956.
- Santin, C., S. H. Doerr, C. M. Preston, and G. Gonzalez-Rodriguez (2015), Pyrogenic organic matter production from wildfires: A missing sink in the global carbon cycle, *Global Change Biol.*, *21*(4), 1621–1633, doi:10.1111/gcb.12800.
- Shen, G. F., et al. (2013), Emission characteristics for polycyclic aromatic hydrocarbons from solid fuels burned in domestic stoves in rural China, *Environ. Sci. Technol.*, *47*(24), 14,485–14,494, doi:10.1021/es403110b.
- Suman, D. O., T. A. J. Kuhlbusch, and B. Lim (1997), Marine sediments: A reservoir for black carbon and their use as spatial and temporal records of combustion, in *Sediment Records of Biomass Burning and Global Change*, edited by J. S. Clark et al., pp. 271–293, Springer, Berlin.
- Sun, X. S., P. A. Peng, J. Z. Song, G. Zhang, and J. F. Hu (2008), Sedimentary record of black carbon in the Pearl River estuary and adjacent northern South China Sea, *Appl. Geochem.*, *23*(12), 3464–3472, doi:10.1016/j.apgeochem.2008.08.006.
- Sun, X. S., M. Hu, S. Guo, K. X. Liu, and L. P. Zhou (2012), ¹⁴C-based source assessment of carbonaceous aerosols at a rural site, *Atmos. Environ.*, *50*, 36–40, doi:10.1016/j.atmosenv.2012.01.008.
- Wang, D. G., F. L. Tian, M. Yang, C. L. Liu, and Y. F. Li (2009), Application of positive matrix factorization to identify potential sources of PAHs in soil of Dalian, China, *Environ. Pollut.*, *157*(5), 1559–1564, doi:10.1016/j.envpol.2009.01.003.
- Wang, F. W., T. Lin, Y. Y. Li, T. Y. Ji, C. L. Ma, and Z. G. Guo (2014), Sources of polycyclic aromatic hydrocarbons in PM_{2.5} over the East China Sea, a downwind domain of East Asian continental outflow, *Atmos. Environ.*, *92*, 484–492, doi:10.1016/j.atmosenv.2014.05.003.

- Wang, F. W., T. Lin, J. L. Feng, H. Y. Fu, and Z. G. Guo (2015), Source apportionment of polycyclic aromatic hydrocarbons in PM_{2.5} using positive matrix factorization modeling in Shanghai, China, *Environ. Sci. Processes Impacts*, *17*(1), 197–205, doi:10.1039/C4EM00570H.
- Wang, X. C., and A. C. Li (2007), Preservation of black carbon in the shelf sediments of the East China Sea, *Chin. Sci. Bull.*, *52*(22), 3155–3161, doi:10.1007/s11434-007-0452-1.
- Wiedemeier, D. B., M. D. Hilf, R. H. Smittenberg, S. G. Haberle, and M. W. I. Schmidt (2013), Improved assessment of pyrogenic carbon quantity and quality in environmental samples by high-performance liquid chromatography, *J. Chromatogr. A*, *1304*, 246–250, doi:10.1016/j.chroma.2013.06.012.
- Wiedemeier, D. B., S. Brodowski, and G. L. B. Wiesenberg (2015a), Pyrogenic molecular markers: Linking PAH with BPCA analysis, *Chemosphere*, *119*, 432–437, doi:10.1016/j.chemosphere.2014.06.046.
- Wiedemeier, D. B., et al. (2015b), Aromaticity and degree of aromatic condensation of char, *Org. Geochem.*, *78*, 135–143, doi:10.1016/j.orggeochem.2014.10.002.
- Wilcke, W. (2007), Global patterns of polycyclic aromatic hydrocarbons (PAHs) in soil, *Geoderma*, *141*(3–4), 157–166, doi:10.1016/j.geoderma.2007.07.007.
- Wilcke, W., M. Kieseewetter, and B. A. Musa Bandowe (2014), Microbial formation and degradation of oxygen-containing polycyclic aromatic hydrocarbons (OPAHs) in soil during short-term incubation, *Environ. Pollut.*, *184*, 385–390, doi:10.1016/j.envpol.2013.09.020.
- Yang, H. H., S. O. Lai, L. T. Hsieh, H. J. Hsueh, and T. W. Chi (2002), Profiles of PAH emission from steel and iron industries, *Chemosphere*, *48*(10), 1061–1074, doi:10.1016/S0045-6535(02)00175-3.
- Yang, Z. S., Y. J. Ji, N. S. Bi, K. Lei, and H. J. Wang (2011), Sediment transport off the Huanghe (Yellow River) delta and in the adjacent Bohai Sea in winter and seasonal comparison, *Estuarine Coastal Shelf Sci.*, *93*(3), 173–181, doi:10.1016/j.ecss.2010.06.005.
- Yunker, M. B., R. W. Macdonald, R. Vingarzan, R. H. Mitchell, D. Goyette, and S. Sylvestre (2002), PAHs in the Fraser River basin: A critical appraisal of PAH ratios as indicators of PAH source and composition, *Org. Geochem.*, *33*(4), 489–515, doi:10.1016/S0146-6380(02)00002-5.
- Zakaria, M. P., H. Takada, S. Tsutsumi, K. Ohno, J. Yamada, E. Kouno, and H. Kumata (2002), Distribution of polycyclic aromatic hydrocarbons (PAHs) in rivers and estuaries in Malaysia: A widespread input of petrogenic PAHs, *Environ. Sci. Technol.*, *36*(9), 1907–1918, doi:10.1021/es011278+.
- Zhang, F., Y. J. Chen, C. G. Tian, X. P. Wang, G. P. Huang, Y. Fang, and Z. Zong (2014), Identification and quantification of shipping emissions in Bohai Rim, China, *Sci. Total Environ.*, *497–498*, 570–577, doi:10.1016/j.scitotenv.2014.08.016.
- Zhang, F., Y. J. Chen, C. G. Tian, J. Li, G. Zhang, and V. Matthias (2015a), Emissions factors for gaseous and particulate pollutants from off-shore diesel engine vessels in China, *Atmos. Chem. Phys. Discuss.*, *15*(17), 23,507–23,541, doi:10.5194/acpd-15-23507-2015.
- Zhang, X. L., S. Tao, W. X. Liu, Y. Yang, Q. Zuo, and S. Z. Liu (2005), Source diagnostics of polycyclic aromatic hydrocarbons based on species ratios: A multimedia approach, *Environ. Sci. Technol.*, *39*(23), 9109–9114, doi:10.1021/es0513741.
- Zhang, Y. L., et al. (2015b), Fossil vs. non-fossil sources of fine carbonaceous aerosols in four Chinese cities during the extreme winter haze episode of 2013, *Atmos. Chem. Phys.*, *15*(3), 1299–1312, doi:10.5194/acp-15-1299-2015.